#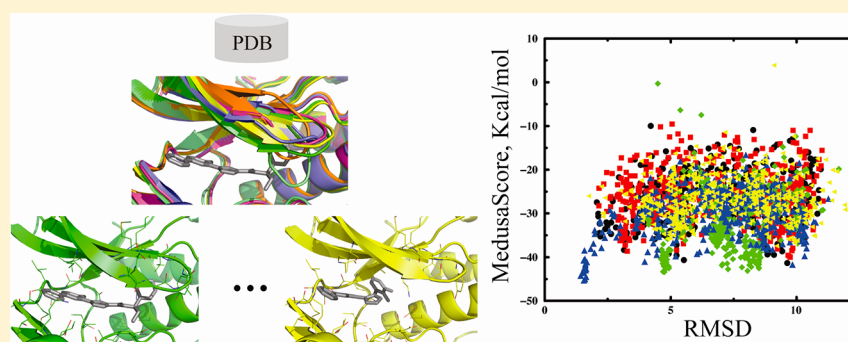 Incorporating Backbone Flexibility in MedusaDock Improves Ligand-Binding Pose Prediction in the CSAR2011 Docking Benchmark

Feng Ding[†,‡] and Nikolay V. Dokholyan*[,‡]

[†]Department of Physics and Astronomy, Clemson University, Clemson, South Carolina 29634, United States
[‡]Department of Biochemistry and Biophysics, University of North Carolina at Chapel Hill, School of Medicine, Chapel Hill, North Carolina 27599, United States

ABSTRACT: Solution of the structures of ligand−receptor complexes via computational docking is an integral step in many structural modeling efforts as well as in rational drug discovery. A major challenge in ligand−receptor docking is the modeling of both receptor and ligand flexibilities in order to capture receptor conformational changes induced by ligand binding. In the molecular docking suite MedusaDock, both ligand and receptor *side chain* flexibilities are modeled simultaneously with sets of discrete rotamers, where the ligand rotamer library is generated "on the fly" in a stochastic manner. Here, we introduce *backbone* flexibility into MedusaDock by implementing ensemble docking in a sequential manner for a set of distinct receptor backbone conformations. We generate corresponding backbone ensembles to capture backbone changes upon binding to different ligands, as observed experimentally. We develop a simple clustering and ranking approach to select the top poses as blind predictions. We applied our method in the CSAR2011 benchmark exercise. In 28 out of 35 cases (80%) where the ligand−receptor complex structures were released, we were able to predict near-native poses (<2.5 Å RMSD), the highest success rate reported for CSAR2011. This result highlights the importance of modeling receptor backbone flexibility to the accurate docking of ligands to flexible targets. We expect a broad application of our fully flexible docking approach in biological studies as well as in rational drug design.

INTRODUCTION

One major challenge in computational prediction of receptor−ligand interactions is the large number of degrees of freedom, including receptor backbone and side chain flexibilities, ligand conformational flexibility, and ligand rigid-body motion. Of particular interest is receptor flexibility, which is essential for capturing the receptor conformational changes upon ligand binding, i.e., the induced-fit effect.[1−5] Receptor induced-fit can be limited to the rearrangement of side chains in the binding pocket, or extended to major rearrangement of the backbone, as observed in many kinases.[6] Because of the high dimensionality in describing receptor conformational changes, modeling receptor flexibility is highly challenging and has been one of the foci of recent ligand−receptor docking studies.[3−5,7−11]

Several approaches have been proposed to capture receptor conformational changes. For example, the generation of an ensemble of multiple predetermined conformations has been proposed to model the receptor flexibility. The receptor conformation ensemble can be obtained experimentally by X-ray crystallography under different conditions or by NMR spectroscopy,[12−15] computationally by molecular dynamics simulations,[7,16−19] comparative modeling,[20] or normal-mode analysis.[11,21] In these approaches, the derivation of structural ensembles representing binding-induced receptor conformational change is *decoupled* from the modeling of ligand binding. Each generated structure of the receptor is kept rigid during ligand docking, and receptor conformational flexibility is realized by selecting the optimal poses from ensemble docking in either sequential (independent)[22] or coupled[23] manners. Therefore, the major challenge to overcome in using these approaches is that the predetermined receptor conformational ensemble must encompass significant sampling such

Table 1. Summary Table of the Predicted Ligand−kinase Poses.[a]

Kinase	Ligand index	Ranked by free energy			Ranked by average energy		
		Pose #1	Pose #2	Pose #3	Pose #1	Pose #2	Pose #3
chk1	1	***0.63***	8.46	3.88	***0.63***	8.46	3.90
	3	***0.77***	10.37	9.81	***0.77***	10.37	9.81
	4	***2.03***	10.33	8.86	***2.03***	10.33	8.86
	6	***0.66***	10.68	10.26	***0.66***	10.68	10.26
	18	***1.84***	6.61	3.48	***1.84***	6.61	3.21
	20	5.84	***1.01***	4.09	5.84	***1.01***	4.09
	24	3.84	***2.09***	4.74	3.84	4.74	***2.09***
	27	7.98	***1.98***	8.07	7.98	9.47	***1.98***
	29	9.03	6.91	4.69	9.03	4.69	6.91
	29*	5.90	***2.27***	8.29	5.90	10.00	6.65
	31	6.36	6.60	***1.27***	***1.27***	6.36	6.60
	34	3.50	3.95	9.27	***0.52***	3.50	8.21
	35	***1.80***	8.97	7.89	7.89	4.04	***1.80***
	36	***1.67***	6.26	6.23	***1.67***	4.78	4.60
	37	***1.12***	6.68	5.88	***1.12***	6.68	5.11
erk2	19	***1.49***	4.71	8.31	4.71	5.24	***1.49***
	20	9.18	4.47	***2.10***	3.19	***1.52***	4.94
	22	***2.26***	7.59	6.30	8.45	***2.26***	8.19
	23	8.62	6.25	4.07	7.22	6.19	4.07
	24	3.92	5.42	4.72	5.42	4.72	7.60
	25	7.19	5.74	5.27	5.88	8.30	4.08
	26	6.52	***1.09***	4.98	***1.09***	6.86	6.52
	27	5.22	5.58	6.59	5.58	4.83	6.59
	32	***2.24***	9.35	6.53	9.35	9.89	9.98
	33	3.45	4.38	5.49	4.38	5.49	5.31
	37	10.26	***2.01***	9.88	6.30	9.23	6.96
	39	5.07	***1.23***	5.89	5.89	6.59	5.07
lpxc	2	***1.33***	12.07	7.19	***1.33***	12.07	11.04
	6	***0.96***	2.52	4.67	***1.23***	2.52	5.05
	7	***1.13***	2.59	10.97	***1.13***	2.59	5.42
	7C	***1.44***	2.73	10.98	***1.44***	2.73	11.04
	13	***1.32***	2.69	5.45	***1.32***	2.69	7.21
urokinase	8	***1.16***	1.94	2.28	***1.16***	1.94	2.28
	12	2.57	***0.52***	2.22	2.57	***0.52***	2.22
	14	***1.26***	5.15	6.37	***1.26***	5.15	6.37
	18	4.52	***0.46***	2.71	***0.46***	4.52	2.71

[a]For each ligand−receptor pair, three poses are submitted for the CSAR 2011 exercise. Two ranking methods, according to either binding free energy or the average binding energy (Methods section), were used. The RMSD values smaller than 2.5 Å are highlighted in italic bold font. The cases where none of the top three poses are within 2.5 Å RMSD are in gray shading. *The given smile of ligand #29 for chk1 was different from the actual ligand. We performed *posterior* docking simulations using the same ligand as observed in the crystal structure.

that the ensemble contains favorable receptor conformations for ligand binding.

Alternative approaches have been proposed to simultaneously sample the receptor and ligand flexibilities during docking.[8−10,24−27] For example, protein side chain rotamer libraries, where continuous protein side chain conformational space is modeled by a set of discrete states,[28] have been used to model protein flexibility during docking.[8,10,24−26] Among these rotamer-based approaches, approaches like RosettaLigand[9,26] and MedusaDock[27] extensively sample receptor side chain conformations near the binding pocket during docking, which has been found to increase the prediction accuracy for near-native poses. Specifically, MedusaDock treats ligand conformational flexibility in the same manner as that of protein side chains, with sets of discrete rotamers. The rotamer library of a ligand is generated in a stochastic manner during docking. Benchmark studies of MedusaDock suggested that sampling protein side chain rotamers together with ligand during docking can efficiently capture the receptor induced-fit, as well as improved virtual screening enrichment for flexible targets.[27]

In this study, we incorporate backbone flexibility into MedusaDock in order to blindly predict the ligand-binding poses

for the CSAR2011 docking benchmark (www.csardock.org), which includes kinase targets known to be highly flexible.[6,8,29,30] We adopt a simple multiple backbone conformation docking approach, where an ensemble of backbone conformations is selected to capture the backbone changes as observed in receptor structures solved under different conditions, including binding with different ligands. We then sequentially dock the ligand to the predetermined backbone conformations using the flexible side chain/flexible ligand docking suite, MedusaDock. We cluster the top-ranked poses generated from flexible docking to each backbone conformation in order to group structurally similar predictions. We score and rank the clusters in order to select the optimal ligand-binding poses for CSAR2011 predictions. Using the flexible backbone docking protocol of MedusaDock, we were able to predict the near-native poses for 28 out of 35 ligands in the CSAR2011 benchmark, the highest success rate of near-native pose predictions (<2.5 Å RMSD), which highlights the importance of modeling receptor backbone in accurate docking of ligands to a flexible target.

■ METHODS

MedusaDock. We use MedusaDock[27] to generate ligand−receptor binding poses. MedusaDock is a flexible docking method,
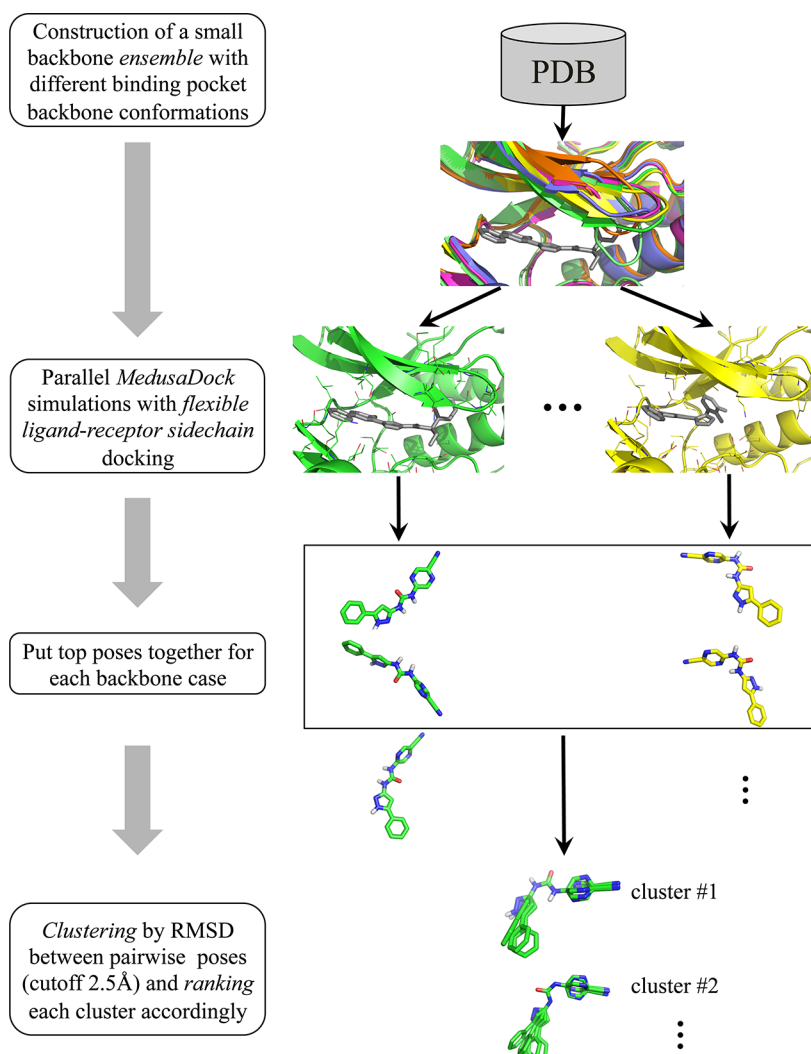
Figure 1. Flowchart of the flexible backbone docking protocol of MedusaDock. The boxes and arrows on the left column summarize the four docking steps (Methods section). The illustrations with protein and/or ligand structures on the right column demonstrate the corresponding steps. Multiple protein backbones in cartoon representation with different colors are selected for independent MedusaDock simulations. The ligands in gray stick are placed in the pocket, where the conformational flexibility of both ligands and receptor side chains (in line representations) are sampled simultaneously. The top poses ranked according MedusaScore are gathered (as shown in the box) for further clustering analysis to group similar poses.

where the flexibilities of ligand and receptor side chains are sampled simultaneously. Details of the docking method can be found in ref.[27] Briefly, a ligand rotamer library is generated in a stochastic manner "on the fly". As a result, the sampling of ligand conformations is treated in a unified way, as in the sampling of protein side chains, which are modeled by a discrete set of conformations, i.e. rotamers.[31,32] The docking protocol is composed of two steps. First, representative ligand conformations are generated by clustering the stochastic rotamer library of each ligand. Each representative ligand conformation is rapidly fitted into a "smoothed" receptor pocket by turning off the van der Waals repulsion between the ligand and the receptor side chains and subsequent rigid-body docking. In the second step, fine-docking is performed from each of the coarsely docked poses, where the binding pose is minimized by iterative repacking of the rotamers of ligand and receptor side chains as well as ligand rigid-body minimization. In the second fine-docking step, the van der Waals repulsions between ligand and receptor side chains are included. We use the MedusaScore[33] scoring function to guide the docking.

MedusaScore. MedusaScore[33] is a physical force field-based scoring function that describes the major physical interactions between proteins and ligands, including the van der Waals interaction (E_{vdw}), hydrogen bonding (E_{hbond}), solvation (E_{solv}), and electrostatics (E_{es}). The van der Waals interaction parameters are adopted from the CHARMM19 force field. We dampen the rapid increase of van der Waals repulsion between overlapping atoms by linear interpolation of the repulsive term of the Lennard–Jones potential.[31] We use the distance and orientation-dependent hydrogen bond model proposed by Kortemme and Baker.[34] We compute the solvation energy using the EEF1 implicit solvent model proposed by Lazaridis and Karplus.[35] The electrostatic interaction is calculated between the formal charges, including the charged residues of arginine, lysine, glutamate, and aspartate in proteins, and identified charged groups in the ligand. We used the distance-dependent dielectric constant, ~r, to model the screening effect. We also introduce a solvent-accessibility-dependent weighting coefficient to model the environmental dependence of the electrostatic interactions.[36]

The total MedusaScore describing the binding is the linear sum of all of these energy terms.

$$E = W_{vdw}E_{vdw} + W_{hbond}E_{hbond} + W_{solv}E_{solv} + W_{es}E_{es} \quad (1)$$

Here, the weights (W) were originally trained and determined for describing interamino acid interactions in high-resolution protein structures.[31] Notably, no protein−ligand data was used in the development of MedusaScore,[33] but the scoring function still exhibits remarkable accuracy in both docking pose discrimination and binding affinity prediction. Therefore, MedusaScore features high transferability in both docking and virtual screening.[27]

Backbone Structural Ensemble Selection. We use the "Sequence Similarity" search functionality included in the protein databank[37] Web site (www.rcsb.org) to identify all solved crystal structures of a protein. Given the reference PDB structures by the CSAR2011 organizers for chk1 (PDB ID: 2e9n), erk2 (PDB ID: 3i5z), lpxc (PDB ID: 3p3e), and urokinase (PDB ID: 1owe) kinases, we identified 62, 10, 4, and 4 solved structures, respectively. Because these ensembles were relatively small and many backbone conformations were very close to each other, we simply aligned all known structures of each kinase and visually identified the representative backbone structures that represented all possible backbone variations in the ligand-binding pocket of those structures using PyMol (www.pymol.org). For large backbone ensembles and also for the purpose of automation, the representative backbones can be selected using clustering analysis.

Clustering. We cluster the ligand poses by root-mean-square deviation (RMSD). Here, we compute the RMSD between two ligands after aligning the two receptors. During the RMSD calculation, we also consider the symmetry of atoms—where a symmetric rotation does not change the physiochemical property of the ligand, such as benzene ring flipping—by taking the lowest deviation among all such symmetric transformations. We use a hierarchical clustering program, oc (www.compbio.dundee.ac.uk/downloads/oc), to group similar poses using a cutoff distance of 2.5 Å. A hierarchical clustering algorithm iteratively joins the two closest clusters into one cluster according to the distances between two clusters. The "cluster distance" is computed based on all pairwise distances between elements of the two corresponding clusters, which can be the minimum, maximum, or the mean of all these values. In this study, we use the mean to compute the distance between two clusters.

Ranking of Clusters. We use two different ranking approaches to rank the clusters. In the first approach, we simply calculate the average MeduaScore

$$\langle E \rangle_c = 1/n_c \sum_i E_i \quad (2)$$

Here, n_c is the cluster size and E_i is the MedusaScore of pose i within a cluster c. In the second approach, we compute the effective free energy of each cluster

$$F_c = \sum_i E_i \exp(-\beta E_i) / \sum_i \exp(-\beta E_i) - k_B T \ln(n_c) \quad (3)$$

Here, β is the reciprocal of $k_B T$, ~0.6 kcal/mol, which corresponds to the thermal fluctuation energy at room temperature (300 K).

■ RESULTS

There were four receptor targets in the CSAR2011 docking benchmark exercise, including checkpoint kinase-1 (chk1),

extracellular-signal-regulated kinase 2 (erk2), N-acetylglucosamine deacetylase from *Pseudomonas aeruginosa* (lpxc), and urokinase. The sequences and reference structures were given by reference to existing experimental structures: chk1 (PDB ID: 2e9n), erk2 (PDB ID: 3i5z), lpxc (PDB ID: 3p3e), and urokinase (PDB ID: 1owe). For each target, ligands were provided in the smile format (47 for chk1, 39 for erk2, 16 for lpxc, and 20 for urokinase; www.csardock.org). The participants were allowed to use any information and methods to model the conformations of the bound complexes. For a subset of these ligands (Table 1), the crystal structures of the ligand−receptor complexes were solved and were used to compare with the blindly predicted poses submitted by the participants.

Flexible Backbone Docking Using MedusaDock. We use MedusaDock[27] to generate ligand-binding poses in a given receptor. MedusaDock models the flexibility of receptor side chains in the pocket but not the receptor backbones (Methods section). To incorporate backbone flexibility for the receptor structures, especially kinases known for large backbone conformational changes upon ligand binding,[6,8,29,30] we develop a simple flexible backbone approach (Figure 1). First, we construct an ensemble of receptor backbone conformations. Because MedusaDock already considers the full receptor side chain flexibility in the binding pocket, which is found to tolerate small backbone variations,[27] we only include a small number of backbone conformations that capture the backbone changes upon ligand binding. We use known receptor structures solved under different conditions to reconstruct the backbone ensemble for each target (Methods section). The backbone ensemble of chk1 includes PDB structures of 2e9u, 2ghg, 2ym4, and 3nle; the ensemble of erk2 includes PDB structures of 1tvo, 1wzy, 2ojg, 3i60, and 3sa0; and the lpxc ensemble includes PDB structures of 2ves, 3p3e, and 3u1y. We find significant backbone variation between the various structures of these flexible receptors (Figure 2). We use
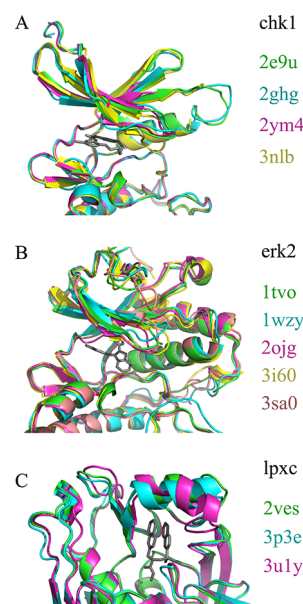

Figure 2. Multi-backbone ensembles for flexible backbone docking. The backbone structures in cartoon representation with different colors are selected from the protein databank for different CSAR2011 receptor targets: (A) chk1, (B) erk2, and (C) lpxc. The PDB IDs for the selected backbone structure are colored accordingly.
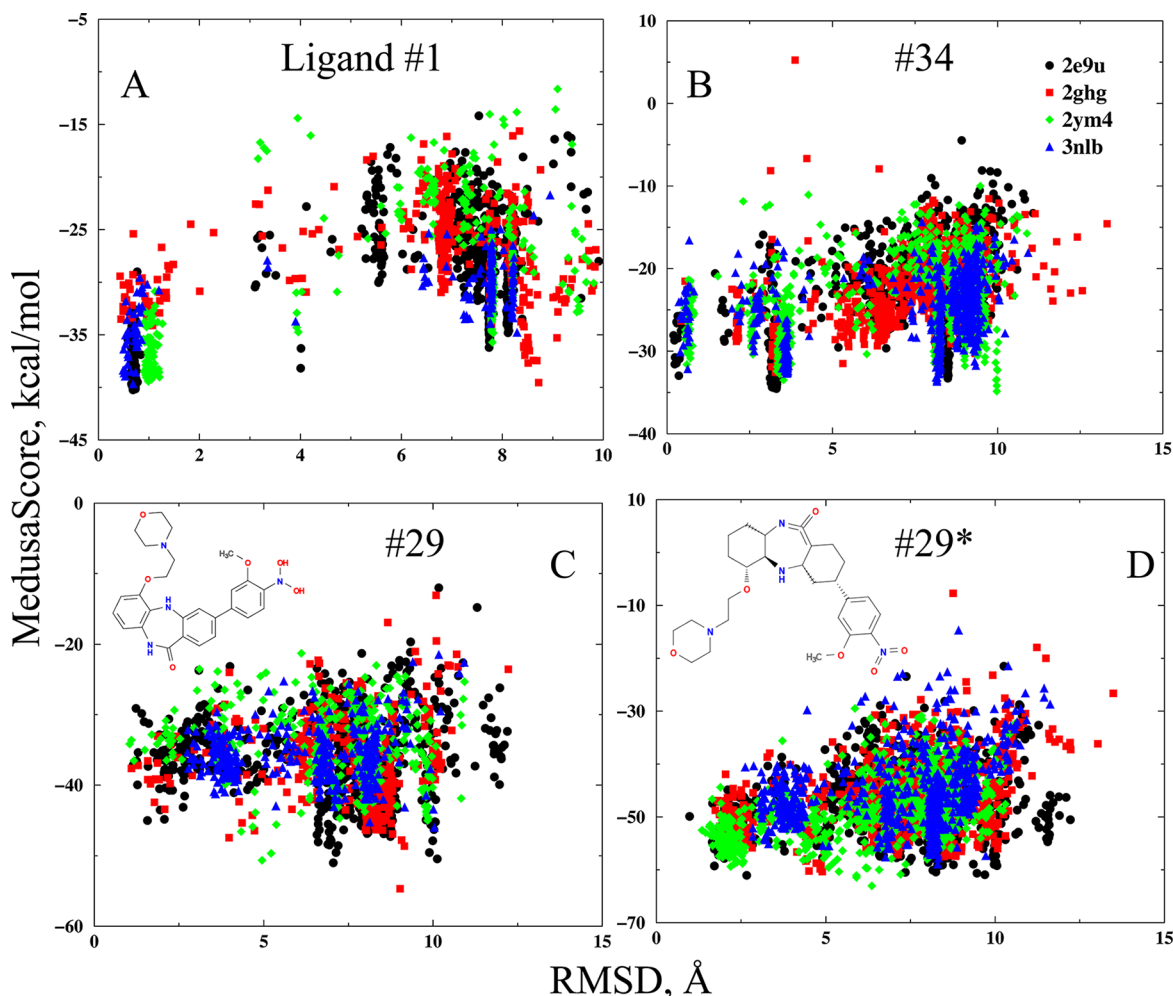
Figure 3. Scatter plot of MedusaScore versus RMSD for chk1 ligand poses. The symbols with different colors denote docking poses generated with different backbone conformations as shown in the legend. Panel (A) and (B) correspond to docking results of ligand #1 and #34, respectively. (C) The results for the docking of ligand #29 that were initially given, which turned out to be different from the released structure. Panel (D) corresponds to the docking result of the actual ligand #29, #29*. The two chemical structures of ligand #29 are given in the corresponding inserts.

only one backbone structure for urokinase (1owe) because all known structures have very similar backbone structures.

Second, for each receptor backbone structure, we perform 100 independent MedusaDock docking simulations. Depending on the number of degrees of freedom of the input ligand, each MedusaDock run generates several poses[27] and takes on average approximately 3−5 min on an Intel 2.6 GHz Xeon processor. All calculations can be done in parallel. Next, we rank all poses for a given receptor backbone conformation according to MedusaScore (Methods section; eq 1). We collect the top N_p poses for a given receptor backbone structure and assemble all selected poses ($N_b N_p$) from N_b backbone structures into a single ensemble for further clustering (Figure 1). Clustering is based on the RMSD between all pairs of poses, the calculation time of which is proportional to ($N_b N_p$)^2. During the CSAR2011 exercise, we restricted $N_p N_b$ to approximately 500 total poses. We group similar poses using a hierarchical clustering approach with a cutoff RMSD of 2.5 Å (Methods section), and each cluster is ranked according to the MedusaScore of poses within the cluster (Methods section). The centroid poses of the top three clusters were submitted as CSAR2011 blind predictions.

Effective Selection of Native Poses Using Free Energy. The CSAR2011 organizers allowed submission of more than

one set of predicted poses, so that specific hypotheses can be tested. We tested two different approaches to score and rank the pose clusters (Methods section). In the first approach, we simply score the cluster by the average MedusaScore (eq 2). In the second approach, we compute the effective free energy of the cluster, where the average potential energy is computed as the Boltzmann-weighted average of the MedusaScore, and the entropy contribution is computed as the logarithm of the cluster size (eq 3). We find that the scoring and ranking using the free energy outperforms that by the average energy (Table 1). In the case of free energy ranking, the lowest RMSD of the predicted three poses is within 2.5 Å for 28 out of 35 (80%) targets. The success rate of the predictions computed from the average energy is 26 out of 35. Therefore, scoring and ranking the clusters by the proposed free energy is a more accurate way to select near-native poses.

Docking with Multiple Backbone Conformations Enriches Native-Like Poses. Our simple flexible backbone docking approach is composed of independent MedusaDock docking simulations with a set of predetermined backbone conformations, and thus, the number of calculations is proportional to the number of structures used. With ensemble docking, we sacrifice additional required computational time in exchange for
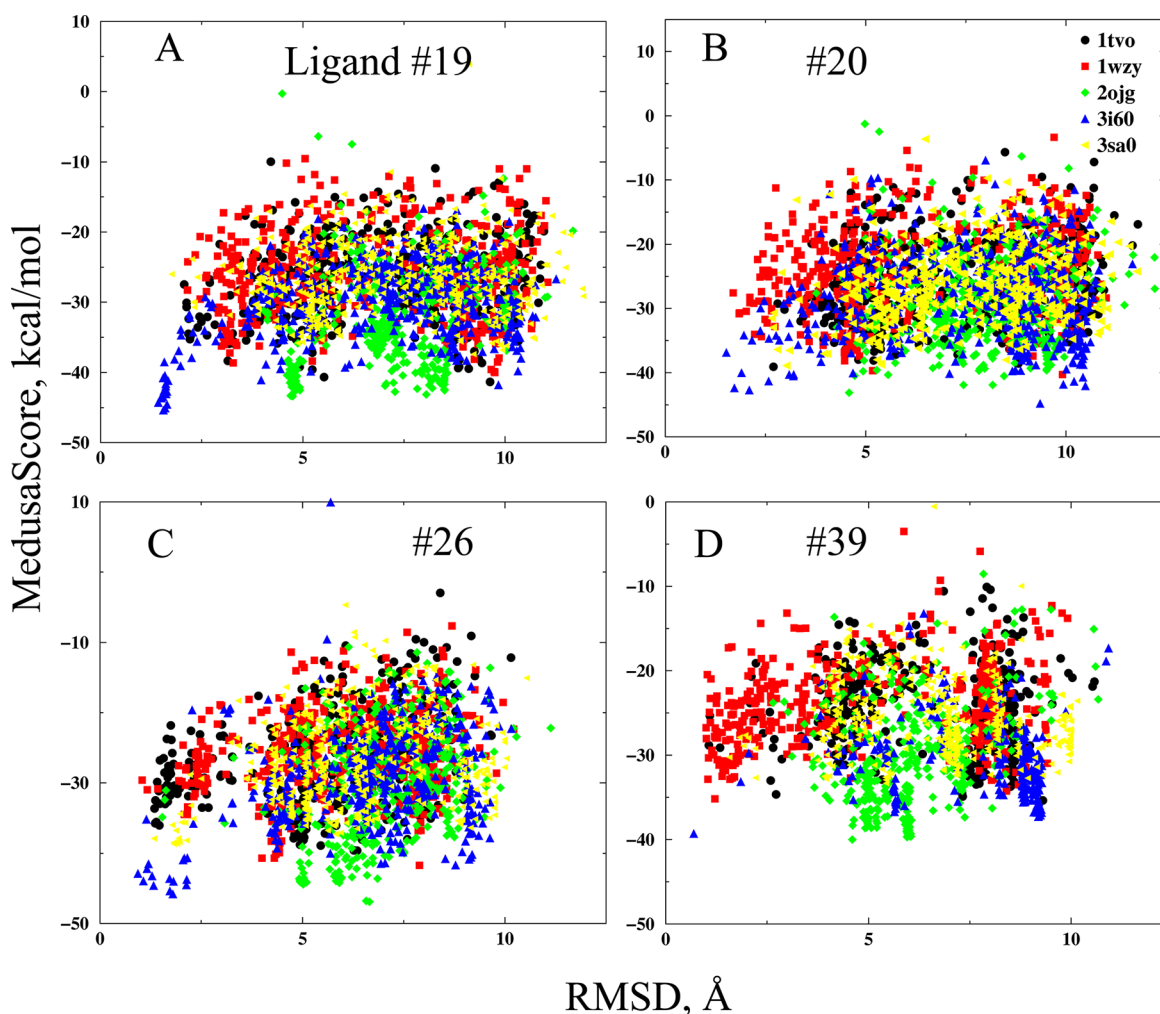
Figure 4. Scatter plot of MedusaScore versus RMSD for erk2 ligand poses. The symbols with different colors denote docking poses generated with different backbone conformations as shown in the legend. Four of the seven success cases are included: ligand #19 (A), #20 (B), #26(C), and #39 (D).

improved prediction accuracy. Next, we discuss the results of docking for each receptor.

chk1. Bound structures have been solved experimentally for chk1 with 14 different ligands (Table 1). Only in two cases (ligand #29 and #34) do our free energy-ranked predictions not succeed in identifying near-native poses. To illustrate the effect of input backbone conformation on pose prediction, we present in Figure 3 the scatter plot of MedusaScore versus RMSD for the poses generated with different backbone conformations. For example, in the case of ligand #1 (Figure 3A), the poses generated from three backbone conformations (2e9u, 2ym4, and 3nlb) feature a funnel-like binding/docking energy land-scape, where the native−native poses have the lowest (most favorable) MedusaScores. However, in the case of backbone conformation of 2ghg, the generated near-native poses have higher (less favorable) MedusaScores than other decoy poses. Taken together, MedusaDock simulations with multiple back-bones enable the accurate prediction of a near-native pose as the top-ranked pose for ligand #1 (Table 1). For the failed case of ligand #34, near-native poses were sampled for all input backbone conformations but all had higher MedusaScores than the decoy poses (Figure 3B). Interestingly, near-native poses of ligand #34 were top-ranked when utilizing the scoring method with average energy (Table 1). *Additionally, we noticed that the chemical*

structure of ligand #29 in the final released structure is different from that provided by the input smile (inserts of Figure 3C,D). We therefore performed flexible docking simulations for the revised structure of ligand #29 after its final release. Although dock-ing to the backbone of 3nlb did not sample near-native states (Figure 3D), the revised ligand structure enabled sufficient sampl-ing of near-native poses when docked to other backbone struc-tures (Figure 3D), achieving a near-native pose as the second-ranked pose (Table 1).

erk2. Twelve erk2-ligand complex structures have been solved experimentally (Table 1). Our method recapitulated near-native poses for seven out of twelve cases. The relatively low success rate compared to chk1 may be a result of high backbone flexi-bility, which is manifested even in the success cases (Table 1; Figure 4). For example, near-native poses were sampled by docking only a small number of backbone conformations (e.g., Figure 4A,B) as compared to chk1 (Figure 3). In other cases, the sampled near-native poses did not have clear separation from decoy poses in terms of MedusaScore (Figure 4B,D). However, using the clustering and ranking approach, we are able to select near-native poses from many decoys in the latter cases. These results (Figure 4), as well as those for chk1 (Figure 3), highlight the importance of incorporating multiple backbone conformations in the sampling of near-native poses with low MedusaScores.
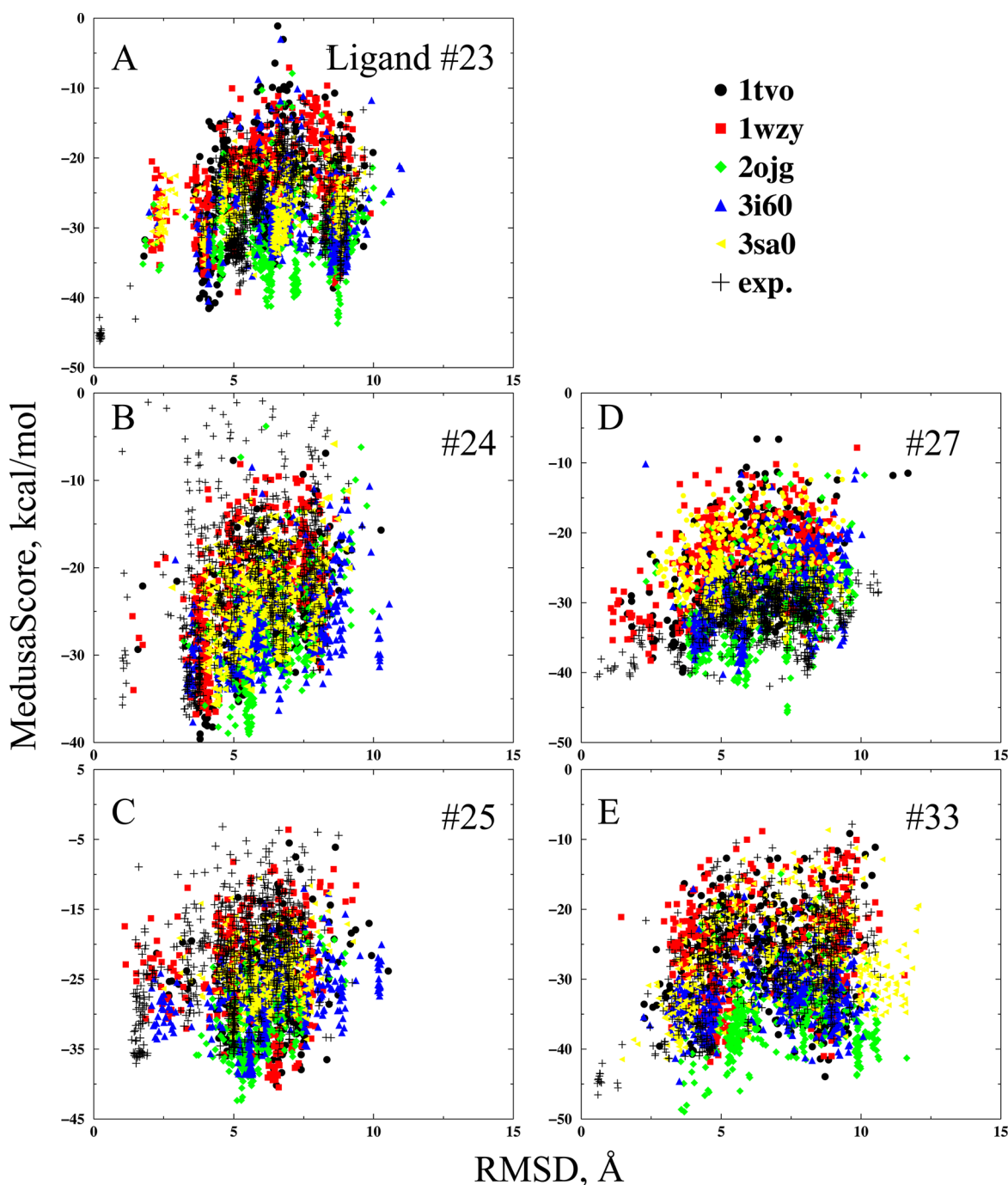
Figure 5. Scatter plot of MedusaScore versus RMSD for erk2 ligand poses. The symbols with different colors denote docking poses generated with different backbone conformations as shown in the legend. Five of the challenging cases are included: ligand #23 (A), #24 (B), #25(C), #27(D), and #33 (E).

In five challenging cases (Figure 5, filled symbols correspond to blind docking results for CSAR2011), the near-native states were either rarely sampled (Figure 5B,E) or sampled but with significantly less favorable MedusaScores than decoys (Figure 5A,C,D). We postulate that the failure to capture near-native states with low MedusaScores is a result of insufficient sampling of backbone conformations in the receptor ensemble. The question is whether docking with the released cocrystallized backbone structure can enrich the near-native poses with low MedusaScores? Therefore, we performed *posterior* MedusaDock simulations with the released backbone conformation. Indeed, the docking with experimentally determined cocrystallized backbone

conformations enables the sampling of near-native poses in all challenging cases (Figure 5, plus symbols). If the cocrystallized backbone structures were included in the predetermined backbone ensemble, the near-native poses of these challenging cases could have been selected by our clustering and ranking method as demonstrated by previous examples (Figures 3,4). Hence, the results of these difficult cases suggest that the sampling of backbone conformation in order to capture the backbone changes upon binding of specific ligands remains a significant challenge.

lpxc and urokinase. The lpxc receptor has a zinc ion as the coligand in all existing structures. We include the zinc ion as a

1877

dx.doi.org/10.1021/ci300478y | *J. Chem. Inf. Model.* 2013, 53, 1871−1879

fixed moiety during MedusaDock simulation. We recapitulate near-native poses for both receptors (Table 1). In the case of lpxc, all top-ranked poses correspond to near-native poses.

■ DISCUSSION AND CONCLUSION

In order to model receptor backbone changes upon ligand binding, we develop a simple multibackbone docking approach using MedusaDock. Because MedusaDock is able to model the full receptor side chain flexibility, we construct a relatively small ensemble of protein backbone conformations for the region near the ligand-binding pocket. The flexible side chain docking approach used by MedusaDock can tolerate small backbone changes, as shown in the previous cross-docking benchmark.[27] For this reason, including a small number of backbone conformations in the ensemble is most computationally efficient because simulation time is directly proportional to the input number of backbone conformations.

The major challenge in ensemble docking is to capture relevant backbone changes upon ligand binding within the predetermined set of backbone configurations. For example, our preconstructed backbone ensembles for chk1, lpxc, and urokinase (Table 1) are able to capture the corresponding backbone changes upon binding of the given ligands, as suggested by the high success rate of prediction of near-native poses (~100%). However, the prediction rate for erk2 kinase is significantly lower because the backbone structures are not well sampled by the constructed backbone ensemble (Figure 5). In the current study, we have utilized crystallographically determined receptor structures solved in complex with different ligands and under different conditions. Protein structural ensembles derived from solution NMR also provides useful information about protein backbone dynamics,[38] which can be used for the flexible docking approach. With the growing number of protein and protein—ligand complex structures deposited into the Protein Data Bank, this approach will have a broad application to drug screening. In cases where a limited number of experimentally solved structures are available, computational modeling of receptor backbone structures can be performed via homology modeling, molecular dynamics, or normal model analysis. The sampling of backbone changes as well as the choice of the optimal number of backbone conformations to use in MedusaDock ensemble docking simulations is a subject for further studies.

We group similar poses using a clustering algorithm and develop a free energy-like scoring method to rank clusters of poses. The new score thus considers both the average MedusaScore of each cluster as well as the cluster size in ranking poses (eq 3). We use a Boltzmann-weighted average of MedusaScores within a cluster to compute the final score, where a pose with a lower (more favorable) MedusaScore has a higher weight. The second term with logarithm of the cluster size also favor the large cluster with many similar poses, corresponding to thermodynamic states with large number of microstates and thus high entropy. Our clustering and ranking approach allows us to select near-native poses even when their scores are not obviously separated from those of decoy poses (e.g., Figures 3D and 4B,D). As the result, we are able to predict the near-native poses for 28 out of 35 ligands, which corresponds to the highest success rate of near-native pose predictions (<2.5 Å RMSD) in the CSAR2011 docking benchmark exercise. We expect a broach application of our fully flexible docking approach in pose prediction for both biological study as well as rational drug design.

■ AUTHOR INFORMATION

Corresponding Author
*E-mail: dokh@med.unc.edu.

Notes
The authors declare no competing financial interest.

■ REFERENCES

(1) Leach, A. R.; Shoichet, B. K.; Peishoff, C. E. Prediction of protein-ligand interactions. Docking and scoring: Successes and gaps. *J. Med. Chem.* **2006**, *49*, 5851−5855.

(2) Sousa, S. F.; Fernandes, P. A.; Ramos, M. J. Protein-ligand docking: Current status and future challenges. *Proteins: Struct., Funct., Bioinf.* **2006**, *65*, 15−26.

(3) Carlson, H. A.; McCammon, J. A. Accommodating protein flexibility in computational drug design. *Mol. Pharmacol.* **2000**, *57*, 213−218.

(4) Teague, S. J. Implications of protein flexibility for drug discovery. *Nat. Rev. Drug Discovery* **2003**, *2*, 527−541.

(5) Teodoro, M. L.; Kavraki, L. E. Conformational flexibility models for the receptor in structure based drug design. *Curr. Pharm. Des.* **2003**, *9*, 1635−1648.

(6) Schindler, T.; Bornmann, W.; Pellicena, P.; Miller, W. T.; Clarkson, B.; Kuriyan, J. Structural mechanism for STI-571 inhibition of abelson tyrosine kinase. *Science* **2000**, *289*, 1938−1942.

(7) Koska, J.; Spassov, V. Z.; Maynard, A. J.; Yan, L.; Austin, N.; Flook, P. K.; Venkatachalam, C. M. Fully automated molecular mechanics based induced fit protein—ligand docking method. *J. Chem. Inf. Model.* **2008**, *48*, 1965−1973.

(8) May, A.; Zacharias, M. Protein—ligand docking accounting for receptor side chain and global flexibility in normal modes: Evaluation on kinase inhibitor cross docking. *J. Med. Chem.* **2008**, *51*, 3499−3506.

(9) Meiler, J.; Baker, D. ROSETTALIGAND: Protein—small molecule docking with full side-chain flexibility. *Proteins: Struct., Funct., Bioinf.* **2006**, *65*, 538−548.

(10) Nabuurs, S. B.; Wagener, M.; de Vlieg, J. A flexible approach to induced fit docking. *J. Med. Chem.* **2007**, *50*, 6507−6518.

(11) Rueda, M.; Bottegoni, G.; Abagyan, R. Consistent improvement of cross-docking results using binding site ensembles generated with elastic network normal modes. *J. Chem. Inf. Model.* **2009**, *49*, 716−725.

(12) Barril, X.; Morley, S. D. Unveiling the full potential of flexible receptor docking using multiple crystallographic structures. *J. Med. Chem.* **2005**, *48*, 4432−4443.

(13) Sheridan, R. P.; McGaughey, G. B.; Cornell, W. D. Multiple protein structures and multiple ligands: Effects on the apparent goodness of virtual screening results. *J. Comput.-Aided Mol. Des.* **2008**, *22*, 257−265.

(14) Knegtel, R. M.; Kuntz, I. D.; Oshiro, C. M. Molecular docking to ensembles of protein structures. *J. Mol. Biol.* **1997**, *266*, 424−440.

(15) Damm, K. L.; Carlson, H. A. Exploring experimental sources of multiple protein conformations in structure-based drug design. *J. Am. Chem. Soc.* **2007**, *129*, 8225−8235.

(16) Cheng, L. S.; Amaro, R. E.; Xu, D.; Li, W. W.; Arzberger, P. W.; McCammon, J. A. Ensemble-based virtual screening reveals potential novel antiviral compounds for avian influenza neuraminidase. *J. Med. Chem.* **2008**, *51*, 3878−3894.

(17) Soliva, R.; Gelpi, J. L.; Almansa, C.; Virgili, M.; Orozco, M. Dissection of the recognition properties of p38 MAP kinase. Determination of the binding mode of a new pyridinyl-heterocycle inhibitor family. *J. Med. Chem.* **2007**, *50*, 283−293.

(18) Karplus, M. Molecular dynamics of biological macromolecules: A brief history and perspective. *Biopolymers* **2003**, *68*, 350−358.

(19) Karplus, M.; Kuriyan, J. Molecular dynamics and protein function. *Proc. Natl. Acad. Sci. U.S.A.* **2005**, *102*, 6679−6685.

(20) Fan, H.; Irwin, J. J.; Webb, B. M.; Klebe, G.; Shoichet, B. K.; Sali, A. Molecular docking screens using comparative models of proteins. *J. Chem. Inf. Model.* **2009**, *49*, 2512−2527.

(21) Keseru, G. M.; Kolossvary, I. Fully flexible low-mode docking: Application to induced fit in HIV integrase. *J. Am. Chem. Soc.* **2001**, *123*, 12708−12709.

(22) Cavasotto, C. N.; Kovacs, J. A.; Abagyan, R. A. Representing receptor flexibility in ligand docking through relevant normal modes. *J. Am. Chem. Soc.* **2005**, *127*, 9632−9640.

(23) Huang, S. Y.; Zou, X. Ensemble docking of multiple protein structures: Considering protein structural variations in molecular docking. *Proteins: Struct., Funct., Bioinf.* **2007**, *66*, 399−421.

(24) Kairys, V.; Gilson, M. K. Enhanced docking with the mining minima optimizer: Acceleration and side-chain flexibility. *J. Comput. Chem.* **2002**, *23*, 1656−1670.

(25) Anderson, A. C.; O'Neil, R. H.; Surti, T. S.; Stroud, R. M. Approaches to solving the rigid receptor problem by identifying a minimal set of flexible residues during ligand docking. *Chem. Biol.* **2001**, *8*, 445−457.

(26) Davis, I. W.; Baker, D. RosettaLigand docking with full ligand and receptor flexibility. *J. Mol. Biol.* **2009**, *385*, 381−392.

(27) Ding, F.; Yin, S.; Dokholyan, N. V. Rapid flexible docking using a stochastic rotamer library of ligands. *J. Chem. Inf. Model.* **2010**, *50*, 1623−1632.

(28) Dunbrack, R. L., Jr.; Karplus, M. Backbone-dependent rotamer library for proteins. Application to side-chain prediction. *J. Mol. Biol.* **1993**, *230*, 543−574.

(29) Bahar, I.; Erman, B.; Jernigan, R. L.; Atilgan, A. R.; Covell, D. G. Collective motions in HIV-1 reverse transcriptase: Examination of flexibility and enzyme function. *J. Mol. Biol.* **1999**, *285*, 1023−1037.

(30) Wang, Y. X.; Freedberg, D. I.; Yamazaki, T.; Wingfield, P. T.; Stahl, S. J.; Kaufman, J. D.; Kiso, Y.; Torchia, D. A. Solution NMR evidence that the HIV-1 protease catalytic aspartyl groups have different ionization states in the complex formed with the asymmetric drug KNI-272. *Biochemistry* **1996**, *35*, 9945−9950.

(31) Ding, F.; Dokholyan, N. V. Emergence of protein fold families through rational design. *PLoS Comput. Biol.* **2006**, *2*, e85.

(32) Yin, S.; Ding, F.; Dokholyan, N. V. Eris: An automated estimator of protein stability. *Nat. Methods* **2007**, *4*, 466−467.

(33) Yin, S.; Biedermannova, L.; Vondrasek, J.; Dokholyan, N. V. MedusaScore: An accurate force field-based scoring function for virtual drug screening. *J. Chem. Inf. Model.* **2008**, *48*, 1656−1662.

(34) Kortemme, T.; Morozov, A. V.; Baker, D. An orientation-dependent hydrogen bonding potential improves prediction of specificity and structure for proteins and protein−protein complexes. *J. Mol. Biol.* **2003**, *326*, 1239−1259.

(35) Lazaridis, T.; Karplus, M. Effective energy function for proteins in solution. *Proteins: Struct., Funct., Bioinf.* **1999**, *35*, 133−152.

(36) Matthew, J. B.; Gurd, F. R. Calculation of electrostatic interactions in proteins. *Methods Enzymol.* **1986**, *130*, 413−436.

(37) Berman, H. M.; Westbrook, J.; Feng, Z.; Gilliland, G.; Bhat, T. N.; Weissig, H.; Shindyalov, I. N.; Bourne, P. E. The Protein Data Bank. *Nucleic Acids Res.* **2000**, *28*, 235−242.

(38) Best, R. B.; Lindorff-Larsen, K.; DePristo, M. A.; Vendruscolo, M. Relation between native ensembles and experimental structures of proteins. *Proc. Natl. Acad. Sci. U.S.A.* **2006**, *103*, 10901−10906.